VII. International Scientific Conference of the Faculty of Transport Engineering
6th – 7th September 2018, Pardubice

MOISTURE INFLUENCE ON THE GPR-MEASURED RDP VALUES OF GRANITE BALLAST UNDER CLEAN AND FOULED CONDITIONS

Salih Serkan ARTAGAN[1], Vladislav BORECKÝ[2], Jaromir BARTOŠ[3], and Robin KUREL[4]

Abstract
Ground Penetrating Radar (GPR) has recently been a routine non-destructive tool in railway infrastructure diagnostics. One of the phenomena occurring in the ballast structure, which can be detected by GPR, is presence of water. Moisture (water) can be trapped more frequently in the fouled railway ballast sections due to the filling of air voids within the ballast by finer materials hence reducing the drainage capability of the track infrastructure. This paper aims at experimentally assessing the moisture influence of the clean and fouled coarse granite ballast on the GPR signal characteristics.

Keywords
ground penetrating radar, railway ballast, moisture, diagnostics, transport infrastructure

1 INTRODUCTION

Railways are regarded as a cost-efficient and secure mode of transport. Diagnosis of the degraded sections of railway infrastructure and developing a good maintenance strategy is the main task of the railway operators in order to provide a sustainable service.

Railway ballast is the pivotal parameter of track infrastructure, condition of which has a key impact on the overall track stability [1]. Ballast fulfils fundamental functions of resisting vertical, longitudinal and lateral stresses applied to sleepers, keeping the track in position and enabling the immediate drainage of water from the track body [1–3]. In this respect, identification of the condition of ballast is significant for decision making process in efficiently assigning the limited funds for maintenance.

Due to cyclic loading from trains and through weathering processes, ballast structure deforms in time. Among many mechanisms, which result in ballast deterioration, ballast fouling and moisture (water) retention within ballast are commonly encountered issues. Ballast fouling, i.e. pollution of ballast occurs when air voids in the ballast are filled with finer materials because of ballast breakdown and infiltration of other materials from the ballast surface or infiltration from the base of the ballast layer [4].

Unless the track is drained adequately, water accumulation takes place in the track body, which subsequently causes a reduction in shear strength and stiffness of ballast as well as

[1] **Ing. Salih Serkan Artagan, Ph.D.,** University of Anadolu, Vocational School of Transport, Eskişehir, Basın Şehitleri Cad. No:152, 26470, Turkey, Phone: +90 222 224 13 91, E-mail: ssartagan@anadolu.edu.tr
[2] **Ing. Vladislav Borecký, Ph.D.,** University of Pardubice, Faculty of Transport Engineering, Studentská 95, Pardubice, 532 10, Pardubice, Czech Republic. Phone: +420 466 036 194, E-mail: vladislav.borecky@upce.cz
[3] **Jaromir Bartoš,** University of Pardubice, Faculty of Transport Engineering, Studentská 95, Pardubice, 532 10, pardubice, Czech Republic. Phone: +420 466 036 183, E-mail: jaromir.bartos@student.upce.cz
[4] **Robin Kurel,** University of Pardubice, Faculty of Transport Engineering, Studentská 95, Pardubice, 532 10, pardubice, Czech Republic. Phone: +420 466 036 183, E-mail: robin.kurel@student.upce.cz

increasing the rate of deterioration and fouling process [5]. Influence of water on fouled ballast is much greater than it is on clean ballast since air voids in clean ballast enable drainage of water whereas in fouled ballast finer particles replacing air voids substantially limit the drainage ability of ballast. Early diagnosis of ballast fouling and trapped water within the ballast is therefore vitally important.

This paper aims at experimentally assessing the moisture influence of the clean and fouled coarse granite ballast on the received GPR signal characteristics.

2 GPR TECHNOLOGY

GPR is a probing technique, which sends discrete pulses of electromagnetic (EM) energy to identify variations of electrical properties of the subsurface [6,7] with a central frequency ranging from 10 MHz to 2.5 GHz to reveal the positions and sizes of electrically different layers and objects [8].

GPR has been in use for about 50 years and it is regarded as a strong non-destructive geophysical method in detecting and visualizing the structural and material features under the surface [9,10].

Particularly with the latest developments of the hardware and software, there has been a steady increase in the interest of both practitioners and researchers in this method lately [9]. GPR method is basically composed of antenna transmission of a radio waves (EM energy) into the ground or another medium via short EM pulses. A portion of the transmitted EM energy is reflected by differences in material relative permittivity (RDP) at material interfaces. Such dissimilarities or so-called anomalies appear in the form of changes in soil layers, groundwater surfaces, or buried objects [10]. In Fig. 1, there is a schematic view of GPR profile generation over ballasted track substructure [11].

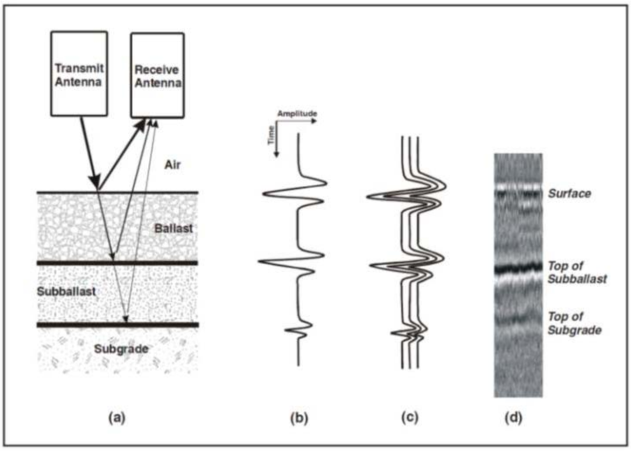

Fig. 1 The generation of a GPR profile with an air-coupled antenna over track bed. a) The transmitted energy is reflected off the boundaries in the substructure, b) A single trace composed of the reflection amplitudes for the reflections in (a), c) Multiple scans are generated in quick succession, d) Adjacent scans are combined to build a B-scan [11].

RDP (or also known as dielectric constant) and the conductivity of a material are the major material properties which govern the transmission and reflection patterns of the EM wave. RDP of a material is the amount of electrostatic energy stored per unit volume for a unit potential gradient by definition [12]. The magnetic susceptibility of a material is assumed not to influence GPR signal significantly [8].

GPR has been used in a great many fields ranging from detection of ice glaciers' thickness to mine detection and from forensic investigations to archeological works. Lately, its potential has been directed to road infrastructure surveys such as pavement layer thickness measurements, detection of voids, layer delamination in bridge deck, measurements of depth to steel dowels, detection of buried objects and utilities, asphalt stripping and scour around bridge piers [8].

A wide spectrum of GPR applications for railway infrastructure has been achieved such as determination of layer (ballast, sub-ballast, subgrade) thicknesses [13], inspection of embankment stability [14, 15], localization of trapped moisture areas within ballast [16], prediction of track modulus from GPR [17], detection of permafrost sections [18–21].

2.1 Known Height Method (KHM)

RDP value (ε_r) of railway ballast provides a preliminary information on the condition of ballast in terms of its fouling level (i.e. clean, fouled, and highly fouled) based on published literature values for that particular type of the ballast. Known Height Method (KHM) was used to compute RDP values in this work. KHM is one of the most common methods to predict RDP values, where the time differences between the reflection amplitudes of air/ballast interface and the ballast/metal plate interface are used. This time difference is widely known as two-way travel time (twt) in GPR glossary. To obtain RDP (ε_r) of ballast, formulas (1) and (2) were used.

$$v_r = \frac{2 \cdot h}{twt} \tag{1}$$

$$\varepsilon_r = \left(\frac{c}{v_r}\right)^2 \tag{2}$$

where v_r is the EM wave velocity through the ballast medium, h is the known height of the ballast layer, *twt* is the two-way radar travel time that the EM wave is transmitted to and reflected back from the target or interface of interest (the ballast layer in this case), ε_r is RDP of railway ballast, c is the speed of light.

3 EXPERIMENTAL FRAMEWORK

Coarse-sized granite ballast and two types of fouling materials (sand and fine-sized gravel) were used to establish the clean and fouled ballast configurations. For clean ballast and for specific levels of fouling (10%, 30%, and 50% of the air voids in ballast) water was added gradually to introduce the moisture effect within the ballast structure according to the air voids volume of the ballast. GPR acquisitions were collected at each increment of water addition to assess the influence of variation of water itself and the combined effect of the changes in fouling and moisture on EM characteristics of the ballast under various conditions. A half-cut Intermediate Bulk Container (IBC) made of HDPE, equipped with a water drain valve, with base sides of 1 m x 1.2 m and a height of 0.50 m, was used during this experiment (Fig. 2). The thickness of the coarse-sized ballast layer was 25 cm. Vertical indicator sticks with height marks on them were used to measure the height of ballast. Placement and compaction of fouling materials were performed appropriately to form an even material layer. Required amounts of fouling materials corresponding to the desired fouling levels were mixed and distributed evenly into the ballast material. Fouling levels from 0% (clean ballast) to 50% (fouled ballast) were gradually arranged for each of the fouling materials at different times. The gradual increase was realized at increments of 10% of the air voids volume within the coarse-sized ballast material. At the first half of the tests, the increments of water were 10% of the air voids, however, then 5% increments were used to better monitor the influence of the addition of the water on the overall system.

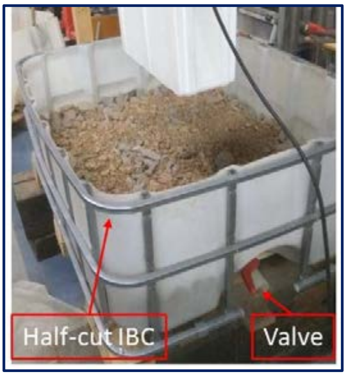

Fig. 2 Half-cut IBC with the drain valve

Air-coupled shielded dipole antenna HN-2000 with central frequency of 2 GHz, which was produced by Ingegneria Dei Sistemi S.p.A. (IDS) (Fig. 3), was used during the experiments. K2 Fast Wave and ReflexW software were utilized for data collecting and for post-processing and the interpretation of the data, respectively.

Fig. 3 Air-coupled 2 GHz horn antenna

Several test configurations such as clean dry, clean wet, fouled dry and fouled wet ballast, are illustrated in Fig. 4.

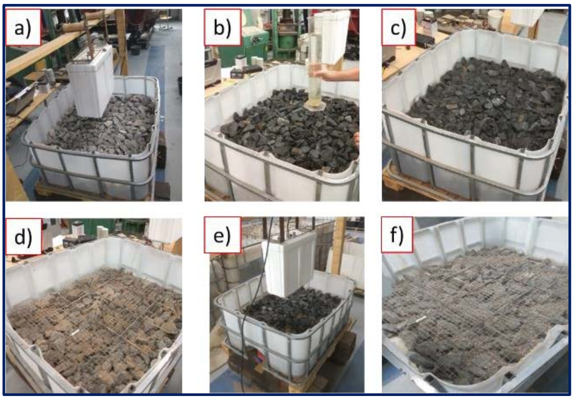

Fig. 4 Test configurations for a) clean dry ballast, b) gradual addition of water to clean ballast via measuring cylinder, c) fully saturated ballast, d) dry ballast fouled with sand, e) wet ballast polluted with sand f) dry ballast fouled with fine gravel

4 RESULTS & DISCUSSION

4.1 Clean Coarse-sized Ballast

The findings for RDP values of gradually water (at 10% increments) included coarser clean ballast are presented in Fig. 5.

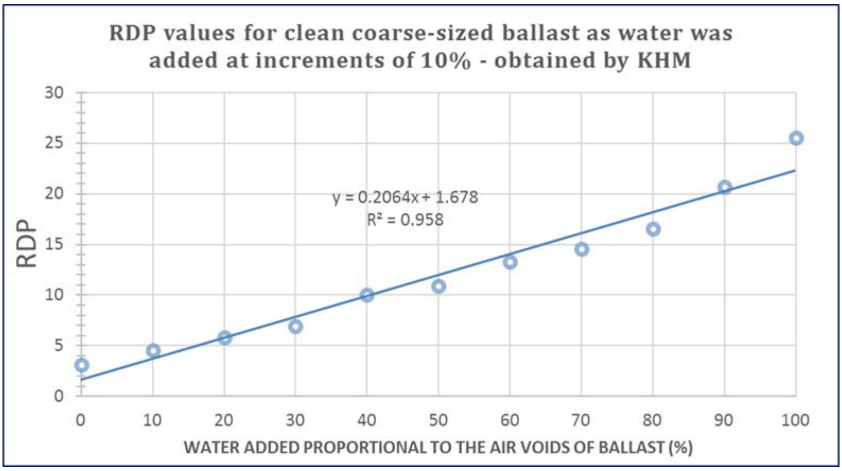

Fig. 5 RDP values for clean coarse-sized ballast at various water contents

At water levels from 0% to 100%, computed RDP values for clean coarse-sized ballast range from 3.090 (no water case) to 25.500 (saturated case). A strong linear trend with the coefficient of determination of 0.958 was observed in Fig. 5. The increase in RDP with increasing water content was also reported by other researchers [3, 22, 23]. After saturation level was reached, GPR data were collected and then water was drained from the IBC. 5 hours after the removal of water, GPR data were collected again. Then, GPR data were acquired in the first, third, sixth, seventh day after discharge of water. Finally, two more tests were carried out in the second and third weeks after removal of water. The corresponding RDP values versus days of GPR measurements are tabulated in Tab. below. RDP of saturated ballast upon the measurement just immediately after water addition was found to be 25.500, which is in line with the results from other studies [3, 22, 23]. GPR data revealed the RDP value of 3.876 just after draining of water. The average value of drained RDP values was 3.152, which is almost the same as the dry clean ballast.

Tab. 1 RDP values vs dry, saturated and drained ballast

Day #	1	2	2	3	5	8	9	16	23
Condition	Dry Clean	Saturated Clean	Just after removal of water (same day)	After 1 day of Removal	After 3 days of Removal	After 6 days of Removal	After 7 days of Removal	After 2 weeks of removal	After 3 weeks of removal
RDP	3.090	25.500	3.876	3.203	3.146	3.146	3.125	3.139	3.150

4.2 Coarse-sized Ballast Fouled by Sand

RDP values were computed for coarse-sized ballast at specific rates of sand fouling namely at 10%, 30%, and 50%. The results are demonstrated in Fig. 6. RDP values for coarse-sized ballast fouled by 10% sand increased from 3.271 to 24.699, as water was added gradually from 0% to 90%, respectively. A strong linear trend with the coefficient of determination of 0.9343 was observed in Fig. 6a. RDP values for coarse-sized ballast fouled by 30% sand are found between

3.538 to 19.774, as water was included progressively from 0% to 70%, respectively. A good linear trend with the coefficient of determination of 0.8939 was observed in Fig. 6b. RDP values for coarse-sized ballast fouled by 50% sand fell into the range from 4.229 to 14.374 as water was added to the IBC step by step from 0% 50% respectively. A strong linear trend with the coefficient of determination of 0.9608 was noted in Fig. 6c.

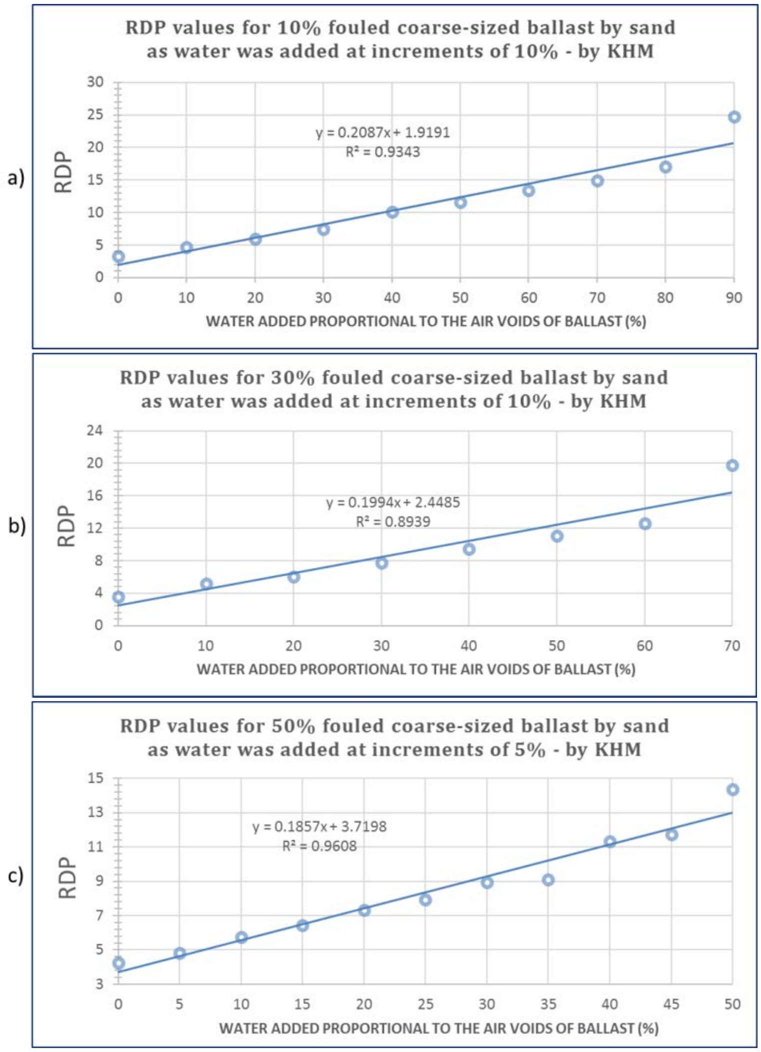

Fig. 6 RDP values for fouled coarse sized granite ballast under gradual water addition at specific levels of sand fouling a) 10%, b) 30%, c) 50% sand fouled ballast

4.3 Coarse-sized Ballast Fouled by Fine-Sized Gravel

Coarse-sized ballast was polluted by gravel at specific percentages of fouling i. e., at 10%, 30%, and 50%. Calculated RDP values are given in Fig. 7. RDP values for coarse-sized ballast fouled by 10% fine gravel range from 3.260 to 16.159, as water was added gradually from 0% to 75%, respectively. It should be noted that after 75% of water addition, no clear reflection from the metal plate was received due to high attenuation. Therefore, the results after 75% water addition were not reported. A strong linear trend with the coefficient of determination of 0.9846 was found in Fig. 7a. RDP values for coarse-sized ballast fouled by 30% fine gravel are computed between

3.523 to 17.650, as water was included progressively from 0% to 70%, respectively. A strong linear relationship with the coefficient of determination of 0.9635 was noted in Fig. 7b. RDP values for coarse-sized ballast fouled by 50% sand ranged from 4.135 to 13.021 as water was added to the IBC step by step from 0% to 50% respectively. A strong linear trend with the coefficient of determination of 0.9978 was noted in Fig. 7c.

a)
b)
c)

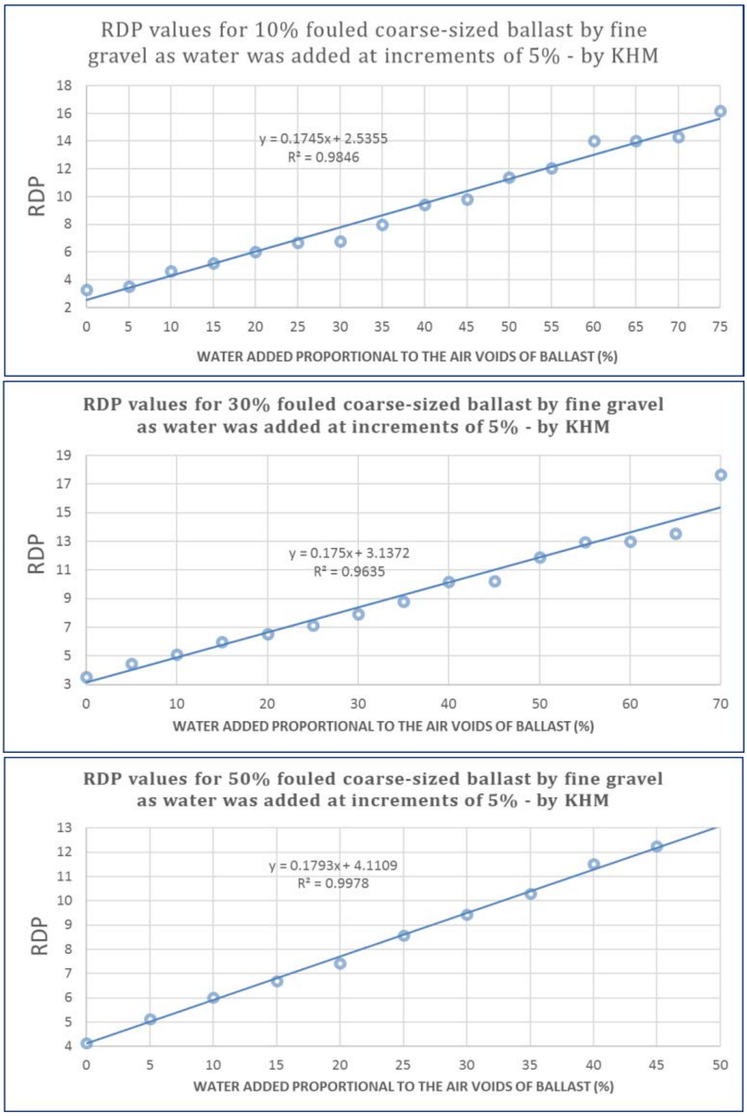

Fig. 7 RDP values for fouled coarse sized granite ballast under gradual water addition at specific levels of fine gravel fouling a) 10%, b) 30%, c) 50% fine gravel fouled ballast

5 CONCLUSION

The influence of moisture (water) in the clean and fouled coarse granite ballast on the GPR signal characteristics are assessed. RDP values of ballast under wet clean and wet fouled conditions by means of KHM were computed. A basis for the prediction of the RDP values of wet clean and wet fouled ballast by comparing the RDP values with the added volumetric percentage of water for a specific fouling level is obtained. Introducing water into clean and fouled ballast increases RDP value meeting the theoretical expectations since the RDP of water is 81.000, which is remarkably higher than the ballast and fouling materials. RDP of saturated clean coarse granite ballast was found to be 25.500, whereas the average value of drained ballast (3.152) was observed to have similar values with the dry one (3.090). For clean ballast and for fouled ballast at each fouling level, increase in the water level led to a rise in RDP values of the mixture of ballast and fouling material. RDP values tend to increase with increasing fouling levels as well. RDP values can be estimated for various water contents by using the linear relationships observed in Figs. 5, 6 and 7.

This research has been realized at the laboratories of Educational and Research Centre in Transport, Faculty of Transport Engineering, University of Pardubice with the GPR set of Department of Transport Structures.

◆◆

Bibliography

[1] SOLOMON, B., Railway Maintenance Equipment: The Men and Machines that Keep the Railroads Running, Voyageur Press, 2001.
[2] AL-QADI, I.L., XIE, W., ROBERTS R., LENG Z., Data analysis techniques for GPR used for assessing railroad ballast in high radio-frequency environment, J. Transp. Eng. 136 (2010) 392–399.
[3] CLARK, M.R., GILLESPIE, R., KEMP, T., McCANN, D.M., FORDE, M.C., Electromagnetic properties of railway ballast, NDT E Int. 34 (2001) 305–311.
[4] ANBAZHAGAN, P., DIXIT, P.S.N., BHARATHA, T.P., Identification of type and degree of railway ballast fouling using ground coupled GPR antennas, J. Appl. Geophys. 126 (2016) 183–190. doi:10.1016/j.jappgeo.2016.01.018.
[5] IBREKK, P.A.Y., Detecting Anomalies and Water Distribution in Railway Ballast using GPR, Norwegian University of Science and Technology (2015).
[6] ROBINSON M., BRISTOW, C., McKINLEY, J., RUFFELL, A., Ground Penetrating Radar, Geomorphological Techniques, Part 1, Sec. 5.5 British Society for Geomorphology, (2013).
[7] NEAL A., Ground-penetrating radar and its use in sedimentology: principles, problems and progress, Earth-Sci. Rev. 66 (2004) 261–330. doi:10.1016/j.earscirev.2004.01.004.
[8] SAARENKETO, T., Electrical properties of road materials and subgrade soils and the use of Ground Penetrating Radar in traffic infrastructure surveys, University of Oulu, 2006.
[9] ANNAN, A.P., DAVIS, J.L., Ground penetrating radar—coming of age at last, in: Proc. Explor., 1997: pp. 515–522. (accessed August 11, 2015).
[10] THOMPSON II, H. B., CARR, G., Ground Penetrating Radar Evaluation and Implementation, Research Results Report, Federal Railroad Administration (2014).
[11] HYSLIP, J. P., Substructure maintenance management – its time has come, in Proceedings of the AREMA Conference, Chicago, 9–12 September 2007.
[12] DE BOLD, R.P., Non-destructive evaluation of railway trackbed ballast, (2011). http://www.era.lib.ed.ac.uk/handle/1842/5027 (accessed September 16, 2015).
[13] FERNANDES F., PEREIRA, M., GOMES CORREIA, A., LOURENÇO, P., CALDEIRA L., Assessment of layer thickness and uniformity in railway embankments with ground penetrating radar, in: E. Ellis, N. Thom, H.-S. Yu, A. Dawson, G. McDowell (Eds.),Adv. Transp. Geotech., CRC Press (2008) pp. 571–575.
[14] SUSSMANN, T.R., SELIG, E.T., HYSLIP, J.P., Railway track condition indicators from ground penetrating radar, NDT E Int. 36 (2003) 157–167.
[15] DONOHUE, S., GAVIN, K., TOLOOIYAN, A., Geophysical and geotechnical assessment of a railway embankment failure, Surf. Geophys. 9 (2011). doi:10.3997/1873-0604.2010040.

[16] HYSLIP, J.P., SMITH, S.S., OLHOEFT G.R., SELIG, E.T., Assessment of railway track substructure condition using ground penetrating radar, in: 2003 Annu. Conf. AREMA, 2003. https://www.arema.org/files/library/2003_Conference_Proceedings/0010.pdf (accessed August 4, 2015).
[17] NARAYANAN, R.M., JAKUB, J.W., LI, D., ELIAS, S.E.G., Railroad track modulus estimation using ground penetrating radar measurements, NDT E Int. 37 (2004) 141–151. doi:10.1016/j.ndteint.2003.05.003.
[18] SAARENKETO, T., SILVAST, M., NOUKKA, J., Using GPR on railways to identify frost susceptible areas, Proc. Int. Conf. Exhib. Railw. Eng., 2003, London.
[19] GUO, Z., DONG, H., XIAO, J., Detection of Permafrost Subgrade Using GPR: A Case Examination on Qinghai-Tibet Plateau, J. Geosci. Environ. Prot. 03 (2015) 35–47. doi:10.4236/gep.2015.35005.
[20] NURMIKOLU, A., Key aspects on the behaviour of the ballast and substructure of a modern railway track: research-based practical observations in Finland, J. Zhejiang Univ. Sci. A. 13 (2012) 825–835. doi:10.1631/jzus.A12ISGT1.
[21] DU, L.Z., ZHANG, X.P., QIU, J.H., LIU, W.B., Study on Ground Penetrating Radar in Detecting of Zero-Temperature Boundary under the Railway Bed, Adv. Mater. Res. 255–260 (2011) 3975–3978. doi:10.4028/www.scientific.net/AMR.255-260.3975.
[22] SUSSMANN, T.R., Application of ground penetrating radar to railway track substructure maintenance management, University of Massachusetts Amherst (1999).
[23] DE CHIARA, F., FONTUL, S., FORTUNATO, E., GPR Laboratory Tests For Railways Materials Dielectric Properties Assessment, Remote Sens. 6 (2014) 9712–9728. doi:10.3390/rs6109712.